Temperature Dependence of the Spin Seebeck Effect in a Mixed Valent Manganite

Avirup De,[1] Arup Ghosh,[1] Rajesh Mandal,[1] Satishchandra Ogale,[1,2] and Sunil Nair[1,2]
[1]Department of Physics, Indian Institute of Science Education and Research, Dr. Homi Bhabha Road, Pune, Maharashtra-411008, India
[2]Centre for Energy Science, Indian Institute of Science Education and Research, Dr. Homi Bhabha Road, Pune, Maharashtra-411008, India

(Received 10 May 2019; revised manuscript received 12 November 2019; published 9 January 2020)

We report on temperature dependent measurements of the longitudinal spin Seebeck effect (LSSE) in the mixed valent manganite $La_{0.7}Ca_{0.3}MnO_3$. By disentangling the contribution arising due to the anisotropic Nernst effect, we observe that in the low temperature regime, the LSSE exhibits a $T^{0.5}$ dependence, which matches well with that predicted by the magnon-driven spin current model. Across the double exchange driven paramagnetic-ferromagnetic transition, the LSSE exponent is significantly higher than the magnetization one, and also depends on the thickness of the spin-to-charge conversion layer. These observations highlight the importance of individually ascertaining the temperature evolution of different mechanisms—especially the spin mixing conductance—which contribute to the measured spin Seebeck signal.

DOI: 10.1103/PhysRevLett.124.017203

The spin Seebeck effect (SSE) [1–4] pertains to the generation of a thermally induced magnonic spin current in a magnetic material subjected to a temperature gradient. The favored means of measuring this spin current is in the form of the longitudinal spin Seebeck effect (LSSE), where a normal metal (NM) with a large spin orbit coupling (typically Pt) is deposited on the magnetic material, and a temperature gradient is applied perpendicular to the plane of the interface [5]. The inverse spin Hall effect (ISHE) enables the conversion of the spin current to a measurable electrical potential difference $E_{\mathrm{ISHE}} \propto \vec{j}_S \times \vec{\sigma}$ (where $\vec{J}_S$ is the spin current density and $\vec{\sigma}$ is the spin polarization of the itinerant electrons in the NM layer) [6]. Junctions comprising of the ferrimagnetic insulator $Y_3Fe_5O_{12}$ (YIG) and Pt are now recognized as being model systems for investigations of the LSSE, and recent measurements have focused on the dependence of the LSSE signals on control parameters like temperature [4,7–9], magnetic field [10,11], and sample thickness [12,13]. Temperature dependent LSSE measurements have also revealed a remarkable correlation of this quantity with intrinsic properties of the magnetic material, and a few strongly correlated systems have been explored in this fashion [14–16].

The investigations of material systems that are not as insulating as YIG are, however, plagued by contaminated SSE signals. These spurious signals arise as a consequence of the anomalous Nernst effect (ANE) in the magnetic subunit as well as the proximity induced ANE in the Pt layer, both of which—by virtue of the geometry of the LSSE—contribute additively to the measured voltage. The disentanglement of these additional contributions from the spin Seebeck signal is clearly imperative for an accurate description of this phenomena. This is especially so, since the agreement between theory and experiments remains tenuous, both in the vicinity of magnetic phase transitions, as well as in the low T regime, where the magnonic spin current is expected to be relatively unaffected by phonons and other associated scattering mechanisms [17,18].

Mixed valent manganites of the form $La_{1-x}A_xMnO_3$ (with A being a divalent alkali metal), where double exchange gives rise to ferromagnetism and concomitant metallicity, are of special interest in spintronics owing to their high spin polarization and colossal magnetoresistance [19]. A prior LSSE measurement on the $La_{0.67}Sr_{0.33}MnO_3$ system suggested that more than 95% of the thermally driven voltage arises from the magnonic spin current contribution alone, with the ANE contribution being barely discernible [16]. However, the disentanglement of the LSSE signal was ambiguous, as evidenced by the fact that measurements with both Pt and W spin-to-charge conversion layers generated signals with the same polarity. In this Letter, we report temperature dependent LSSE measurements of the closely related $La_{0.7}Ca_{0.3}MnO_3$ system, where our data provide critical insight into the functional form of the LSSE—especially at low temperatures and in the vicinity of the magnetic phase transition.

A popular means of disentangling the intrinsic LSSE from both the possible spurious ANE contributions has been the use of a nonmagnetic spacer layer between the ferromagnet and the NM [20–22], albeit at the risk of attenuating the LSSE voltages [12,23]. Recently, a quantitative disentanglement of the SSE from these spurious ANE contributions was reported [24]. Using a set of Pt-$NiFe_2O_x$/$Ni_{33}Fe_{67}$ bilayers (with sample resistances varying across 7 decades)

and utilizing in-plane and out-of-plane measurement geometries, it was demonstrated that the proximity-induced ANE was a contributory factor only in the most metallic of specimens (with $\rho \approx 10^{-7}\ \Omega\,\mathrm{m}$). Since manganites are known to be *dirty* metals (with resistivities of the order of $10^{-4}\ \Omega\,\mathrm{m}$), a contamination of the LSSE signals by the proximity-induced ANE is unlikely in our case.

To disentangle the ANE and LSSE contributions, measurements were done in the standard LSSE geometry [Figs. 1(a) and 1(b)] on both a bare LCMO film and LCMO-Pt (or LCMO-W) bilayer. 200 nm thick epitaxial thin films of the nominal composition $La_{0.7}Ca_{0.3}MnO_3$ were grown on a $LaAlO_3$ (100) substrate using pulsed laser deposition, and a Pt (5/10 nm) or a W (13 nm) film was coated on top of the magnetic layer using dc sputtering. The voltage measured across the bare LCMO film comprises of the ANE alone (V_{ANE}), whereas that measured across the bilayer (V_{Total}) is a sum of the intrinsic magnonic contribution (V_{LSSE}) and the spurious contribution due to the ANE in the LCMO film (V_{ANE}). Since these voltages are measured across different effective resistances, we report all the voltages in their normalized form, i.e., $V_i = V_T/(R_T \Delta T L_y)$, where V_T is the measured transverse voltage, R_T is the corresponding resistance between contact probes, L_y is the distance between contact probes, and the index i refers to the ANE, Total, or LSSE voltages (see Supplemental Material [25] for more details). Figure 1(c) depicts the hysteresis in these signals as a function of varying magnetic fields at a mean sample temperature of 105 K. The linearity of the measured voltages as a function of ∇T with the cold end of the specimen being fixed at 100 K and the magnetic field at 1 kOe is shown in Fig. 1(d). The magnitude and the sign of the measured V_{LSSE} with the Pt and W spin-to-charge conversion layers are commensurate with the experimentally determined spin Hall angles of these heavy metals [30]—confirming the intrinsic nature of the inferred LSSE signals.

The temperature dependence of the magnetization (M), the resistivity (ρ), and the individual ANE and LSSE contributions for two LCMO/Pt devices are depicted in Fig. 2. Our LCMO specimen exhibits a double-exchange driven paramagnetic-ferromagnetic phase transition at 258 K, which is consistent with reports in bulk and thin film specimens of this composition [31,32]. We observe a slight reduction in the magnitude of LSSE signals as a function of decreasing Pt thickness, which is also consistent with prior reports on YIG/Pt bilayers [33,34]. In similarity to that reported in other systems, a peak in $V_{\mathrm{LSSE}}(T)$ is also

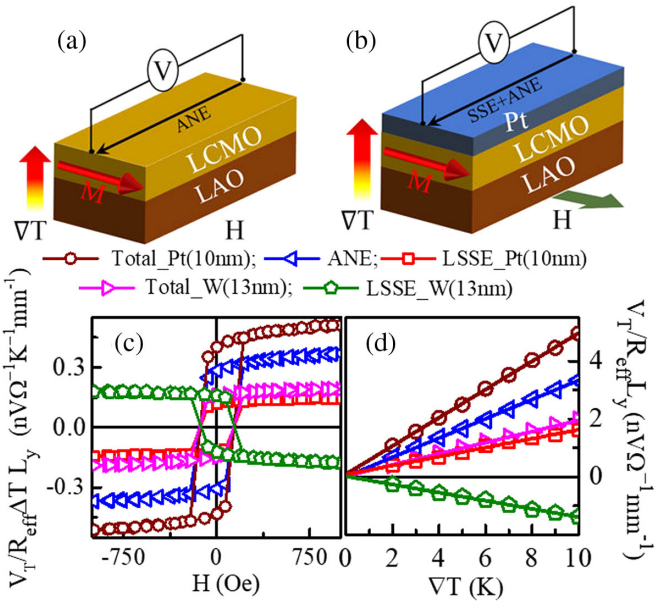

FIG. 1. (a) and (b) Schematic illustrations of the device for measuring the ANE and the total signal (LSSE + ANE), respectively. (c) and (d) The H and ∇T dependence of these signals with a 10 nm Pt and a 13 nm W overlayer. The linearity as a function of ∇T and the reversal of the sign of the LSSE between the Pt and W layers confirms the intrinsic nature of the measured spin Seebeck signal.

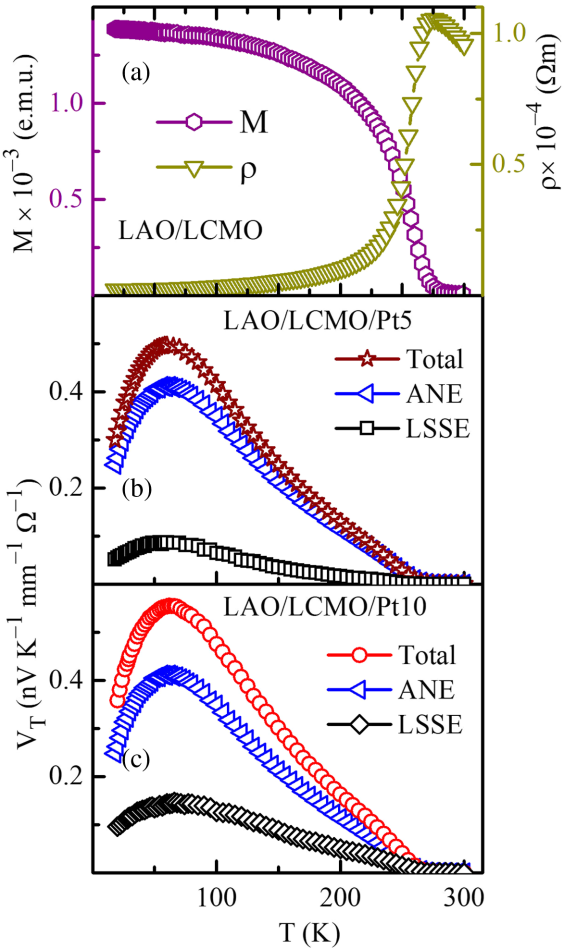

FIG. 2. (a) The temperature dependence of the magnetization and the resistivity of the bare LCMO film. (b) and (c) The temperature dependence of the total, ANE and LSSE signals as measured on devices with Pt thickness of 5 and 10 nm, respectively.

observed at lower temperatures. This peak deep within the magnetically ordered regime is a defining feature of all T dependent measurements of the LSSE and is suggested to arise as a consequence of the T dependence of the magnon relaxation rates and population [8,13].

Theoretical descriptions of the magnon-driven spin Seebeck effect have relied on the mechanism of spin pumping caused by a finite difference between the effective magnon temperature in the ferromagnetic material and the electron (and phonon) temperature in the NM Pt layer. First proposed in the context of the transverse measurement geometry [35], this model was later modified for the LSSE geometry by Rezende and co-workers [36]. On an application of a thermal gradient $\vec{\nabla}T$, the spin current density ($\vec{J}_s$) flowing through the interface is given by $\vec{J}_s = D_s\vec{\nabla}T$. The spin Seebeck coefficient (D_s) has the form $D_s = \gamma\hbar k_B g^{\uparrow\downarrow}/(2\pi M_s V_a)$, where γ, $\hbar$, $g^{\uparrow\downarrow}$, k_B, M_s, and V_a refer to the gyromagnetic ratio, the Planck constant, the spin mixing conductance, the Boltzmann constant, the saturation magnetization, and the magnetic coherence volume, respectively [35]. The temperature dependence of this spin current is thus primarily expected to arise as a consequence of the T dependence of the magnetic coherence volume [$V_a = [2/(3\zeta\frac{5}{2})](4\pi/K_B)(D/T)^{\frac{3}{2}}$, with ζ being the Riemann Zeta function and D the spin stiffness constant], implying that $J_S \propto (g^{\uparrow\downarrow}/M_s)(T/D)^{\frac{3}{2}}$. This spin current flows into the Pt layer, with a spin diffusion length λ_{Pt} and generates a charge current $\vec{J}_c = (2e/\hbar)\theta_{\mathrm{Pt}}\vec{J}_c \times \vec{\sigma}$,where e, θ_{Pt}, and σ refer to the electronic charge, spin Hall angle of Pt, and spin polarization of the conduction electrons in Pt, respectively [6]. The corresponding SSE voltage is given by $V_{\mathrm{LSSE}} = R_d l_{\mathrm{Pt}}\lambda_{\mathrm{Pt}}(2e/\hbar)\theta_{\mathrm{Pt}}\tanh(t_{\mathrm{Pt}}/2\lambda_{\mathrm{Pt}})J_s$, where R_d, l_{Pt}, and t_{Pt} are the resistance between the contacts across Pt, length of the Pt bar, and thickness of the Pt layer, respectively [36,37]. Since $\tanh(t_{\mathrm{Pt}}/2\lambda_{\mathrm{Pt}}) \approx 1$ in our case, and with $\lambda_{\mathrm{Pt}} \propto T^{-1}$ [38] and M_s being invariant at low temperatures, $V_{\mathrm{LSSE}} \propto [(\theta_{\mathrm{Pt}}g^{\uparrow\downarrow}T^{\frac{1}{2}})/(D^{\frac{3}{2}})]$—implying that V_{LSSE} should vary as $T^{0.5}$, at least at low temperatures. However, prior measurements on the model YIG-Pt system have revealed a linear T dependence, which has been attributed to the quadratic magnon dispersion in YIG [8], and on the influence of the thermal conductivity in determining the functional form of V_{LSSE} [7].

Figure 3 depicts an expanded view of the T dependence of V_{LSSE} as measured in the LCMO-Pt bilayers at low temperatures. We observe that at the lowest temperatures, V_{LSSE} varies approximately as $T^{0.5}$—an observation which is in good agreement with the spin magnon theory. We also note that the LSSE exponent is nearly invariant as a function of Pt thickness. With the proximity induced ANE being reported to exhibit a pronounced dependence on the thickness of the NM Pt layer [39,40], this observation confirms that a contamination of the LSSE signals by the proximity-induced ANE can be ruled out in our case.

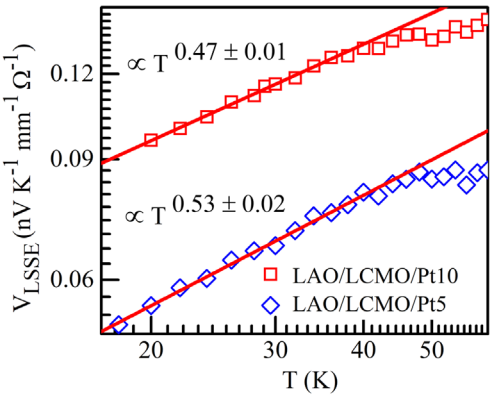

FIG. 3. The temperature dependence of V_{LSSE} at temperatures below 60 K. In the region where ΔT_{eff} remains invariant, the LSSE signal varies as 0.47 ± 0.01 and 0.53 ± 0.02 in LAO/LCMO/Pt devices with Pt thickness of 10 and 5 nm, respectively.

Since the magnon driven spin current is proportional to the effective temperature gradient (ΔT_{eff}) across the LCMO layer, it is important to estimate how this quantity varies in this temperature range. Using literature values of the thermal conductivity of LCMO [26] and LAO [27], we estimate the variation in ΔT_{eff} in the case of the LCMO/LAO (and a LCMO/STO) bilayer (see Supplemental Material [25]), and observe that this $T^{0.5}$ form is observed only in the regime in which ΔT_{eff} is nearly invariant. It has been suggested earlier that the low energy (or subthermal) magnons contribute disproportionately to the measured V_{LSSE} signal, and that phonon mediated magnon scattering needs to be explicitly considered in describing the magnitude as well as the T and H dependence of the LSSE [10,17]. Prior work on YIG-Pt devices has also suggested an intimate coupling between the thermal conductivity (κ) and the measured V_{LSSE}, reinforcing the importance of phonon-mediated processes in the LSSE [7]. The fact that at higher temperatures, our V_{LSSE} signals deviate from $T^{0.5}$ indicates that an inordinate change in ΔT_{eff} across the magnetic LCMO film provides the upper bound for observing the theoretically expected functional form of V_{LSSE}.

Theory and experiments have also failed to reconcile with regard to the functional form of the SSE near the magnetic phase transition. The only prior measurements on YIG-Pt devices have reported that the SSE signal varied as $(T_c - T)^3$ [4] or as $(T_C - T)^{1.5}$ [9] in the vicinity of the magnetic phase transition, whereas the magnetization scaled as $(T_c - T)^{0.5}$, as is expected from mean field theory. However, subsequent theoretical investigations have predicted that the SSE should vary in consonance with the magnetization. For instance, an atomic numerical simulation considering the full spin wave spectrum of the ferrimagnetic YIG suggested that the SSE should have the same exponent as the magnetization [41]. A time dependent Ginzburg-Landau analytical treatment of a

(simple single-sublattice) ferromagnet also suggested that the SSE signal should vary along with the magnetization as $(T_c - T)^{0.5}$ [42]. Figures 4(a) and 4(b) depict the temperature dependence of both the $M(T)$ as well as the $V_{\mathrm{LSSE}}(T)$ in the vicinity of the para-ferromagnetic phase transition in LCMO. We obtain a critical exponent of 0.357 ± 0.003 for the magnetization which is in good agreement with previous reports [43,44]. Interestingly, in the same region we obtain an exponent of 0.64 ± 0.01 and 1.25 ± 0.03 for the $V_{\mathrm{LSSE}}(T)$ with Pt thicknesses of 10 and 5 nm, respectively. It was speculated that the difference between the magnetization and LSSE exponents in the case of YIG/Pt could arise as a consequence of the *ferri*magnetic nature of YIG, or other considerations, like the magnetic surface anisotropy [42]. Though spin wave spectra are expected to be material specific, the fact that we observe a similar discrepancy between the magnetization and LSSE exponents in the case of LCMO/Pt indicates this could be a generic feature of the LSSE signals in the vicinity of a magnetic phase transition.

This difference in the M and V_{LSSE} critical exponents could be a consequence of the fact that the LSSE signal is not only a function of the static magnetic properties of the ferromagnet, but would also be determined by the T dependence of other factors like the spin mixing conductance, the spin-diffusion length, and the spin-Hall angle of the NM layer [4]. We note that the intrinsic spin Hall angle of Pt is reported to be invariant in the temperature range of the LCMO transition [45], and hence is unlikely to be a contributory factor. It has also been demonstrated earlier that the spin diffusion length of Pt is nearly invariant in the temperature range of the LCMO phase transition [38,45]. The magnon-driven spin current density is expected to vary inversely with the magnetic coherence volume (V_a), which in turn has a $D^{3/2}$ dependence (with D being the spin stiffness coefficient). Interestingly, it has been reported that in LCMO this spin stiffness coefficient has an anomalous T dependence in the vicinity of the phase transition and does not fall to zero as $T \to T_c$ [46]. This is presumably due to the finite magnetic correlations in the paramagnetic phase—a hallmark of the colossal magnetoresistive manganites. However, the anomalous T dependence of the magnetic coherence volume (V_a), as well as the effective temperature gradient (ΔT_{eff}) should be similar for both the films depicted in Fig. 4(b). The fact that we observe a pronounced increase in the LSSE exponent as a function of decreasing Pt thickness suggests that the temperature dependence of the spin momentum transfer at the interface could be responsible for this anomalous temperature dependence of the LSSE signal.

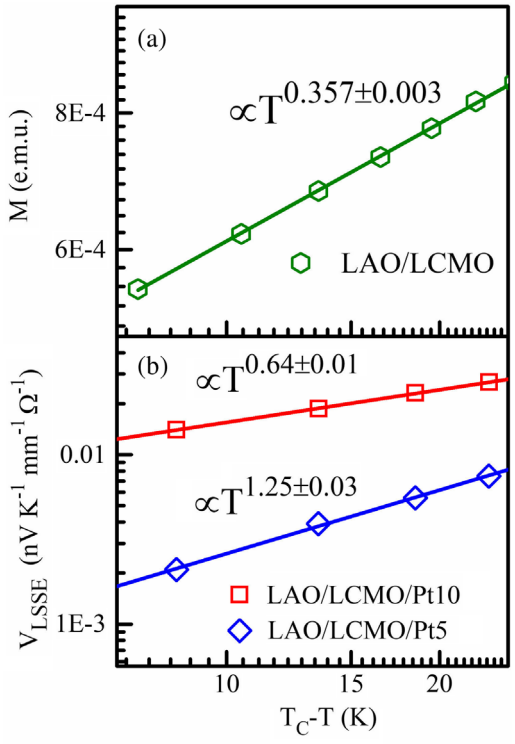

FIG. 4. The $T_C - T$ dependence of the magnetization and the LSSE signals are depicted in (a) and (b), respectively. The critical exponent of V_{LSSE} is seen to be much larger than that of the magnetization, and also varies with the thickness of the Pt spin-to-charge conversion layer.

Prior ferromagnetic resonance (FMR) investigations on a LCMO film of similar composition have reported a pronounced change in the FMR linewidth (ΔH) across the para-ferromagnetic phase transition [47]—implying a change in the Gilbert damping(α) since $\alpha = (\gamma \Delta H/2\omega)$, with γ and ω being the gyromagnetic ratio and the microwave frequency, respectively. The spin mixing conductance being related to the Gilbert damping through the relation $g_r^{\uparrow\downarrow} = (4\pi M_S d_f/g\mu_\beta)\Delta\alpha$ (with M_S, d_f, and g being the spontaneous magnetization, film thickness, and Lande g factor, respectively) [48,49], would thus be expected to have a significant influence on the observed V_{LSSE} exponent. Interestingly, previous reports have also revealed that the effective $g_r^{\uparrow\downarrow}$ (or $\Delta\alpha$) depends on parameters like the quality of the interface [50] and the thickness of the Pt layer [51–53]. Since we observe a twofold increase in the V_{LSSE} exponent as a function of decreasing Pt thickness, it is reasonable to infer that $g_r^{\uparrow\downarrow}(T)$ plays a critical role in determining the functional form of V_{LSSE} in the vicinity of the magnetic phase transition. This temperature dependence of the spin mixing conductance could also probably explain why our measured $V_{\mathrm{LSSE}}(T)$ matches well with the magnon-driven spin current model in the low-T regime, whereas model systems like YIG-Pt do not exhibit this behavior. Recent ferromagnetic resonance (FMR) measurements on YIG have indicated a pronounced T dependence of the FMR linewidth (ΔH), implying a change in the Gilbert damping (α) and, consequently, the spin mixing conductance at low temperatures [54]. On the other hand, early FMR measurements on $La_{0.7}Ca_{0.3}MnO_3$ have indicated that ΔH is

relatively T independent below 100 K [47], suggesting that it is this relative T invariance of the spin mixing conductance and other parameters (like D and θ_{Pt}) that allows us to observe the theoretically predicted $T^{0.5}$ dependence of $V_{LSSE}(T)$ in the low temperature regime.

In summary, we report on temperature dependent measurements of the LSSE on an optimally doped $La_{0.7}Ca_{0.3}MnO_3$ system. After disentangling the ANE contribution we observe that in the low T regime, $V_{LSSE}(T)$ varies as $T^{0.5}$, as is expected by the magnon-driven spin current model. In the para-ferromagnetic transition region, the V_{LSSE} exhibits an exponent which is much larger than that of the magnetization—a feature which could be generic to most phase transitions of this nature. This exponent is also seen to vary with the thickness of the Pt layer, indicating that a temperature dependent spin mixing conductance plays an important role in the measured $V_{LSSE}(T)$. Our observations reinforce the need to individually ascertain the T dependencies of contributory mechanisms—especially the spin mixing conductance—which play a role in dictating both the magnitude of spin current as well as the extent of spin to charge conversion to understand the temperature dependent LSSE in strongly correlated materials.

S. N. is grateful to S. Ramakrishnan for his support. A. D. acknowledges UGC, Government of India for providing financial support through a Senior Research Fellowship. A. G. acknowledges SERB, DST, Government of India for providing the financial support through a National Post-Doctoral Fellowship (PDF/2015/000599). The authors acknowledge funding support by the Department of Science and Technology (DST, Government of India) under the DST Nanomission Thematic Unit Program (SR/NM/TP-13/2016).

[1] K. Uchida, S. Takahashi, K. Harii, J. Ieda, W. Koshibae, K. Ando, S. Maekawa, and E. Saitoh, Nature (London) **455**, 778 (2008).
[2] K. Uchida, J. Xiao, H. Adachi, J.-i. Ohe, S. Takahashi, J. Ieda, T. Ota, Y. Kajiwara, H. Umezawa, H. Kawai *et al.*, Nat. Mater. **9**, 894 (2010).
[3] K.-i. Uchida, H. Adachi, T. Ota, H. Nakayama, S. Maekawa, and E. Saitoh, Appl. Phys. Lett. **97**, 172505 (2010).
[4] K.-i. Uchida, T. Kikkawa, A. Miura, J. Shiomi, and E. Saitoh, Phys. Rev. X **4**, 041023 (2014).
[5] D. Meier, D. Reinhardt, M. Van Straaten, C. Klewe, M. Althammer, M. Schreier, S. T. Goennenwein, A. Gupta, M. Schmid, C. H. Back *et al.*, Nat. Commun. **6**, 8211 (2015).
[6] E. Saitoh, M. Ueda, H. Miyajima, and G. Tatara, Appl. Phys. Lett. **88**, 182509 (2006).
[7] R. Iguchi, K.-i. Uchida, S. Daimon, and E. Saitoh, Phys. Rev. B **95**, 174401 (2017).
[8] H. Jin, S. R. Boona, Z. Yang, R. C. Myers, and J. P. Heremans, Phys. Rev. B **92**, 054436 (2015).
[9] S. Wang, L. Zou, X. Zhang, J. Cai, S. Wang, B. Shen, and J. Sun, Nanoscale **7**, 17812 (2015).
[10] T. Kikkawa, K.-i. Uchida, S. Daimon, Z. Qiu, Y. Shiomi, and E. Saitoh, Phys. Rev. B **92**, 064413 (2015).
[11] U. Ritzmann, D. Hinzke, A. Kehlberger, E.-J. Guo, M. Kläui, and U. Nowak, Phys. Rev. B **92**, 174411 (2015).
[12] A. Kehlberger, U. Ritzmann, D. Hinzke, E.-J. Guo, J. Cramer, G. Jakob, M. C. Onbasli, D. H. Kim, C. A. Ross, M. B. Jungfleisch *et al.*, Phys. Rev. Lett. **115**, 096602 (2015).
[13] E.-J. Guo, J. Cramer, A. Kehlberger, C. A. Ferguson, D. A. MacLaren, G. Jakob, and M. Kläui, Phys. Rev. X **6**, 031012 (2016).
[14] R. Ramos, T. Kikkawa, K. Uchida, H. Adachi, I. Lucas, M. Aguirre, P. Algarabel, L. Morellón, S. Maekawa, E. Saitoh *et al.*, Appl. Phys. Lett. **102**, 072413 (2013).
[15] S. Geprägs, A. Kehlberger, F. Della Coletta, Z. Qiu, E.-J. Guo, T. Schulz, C. Mix, S. Meyer, A. Kamra, M. Althammer *et al.*, Nat. Commun. **7**, 10452 (2016).
[16] B. Wu, G. Luo, J. Lin, and S. Huang, Phys. Rev. B **96**, 060402(R) (2017).
[17] I. Diniz and A. Costa, New J. Phys. **18**, 052002 (2016).
[18] S. R. Boona, New J. Phys. **18**, 061002 (2016).
[19] M. B. Salamon and M. Jaime, Rev. Mod. Phys. **73**, 583 (2001).
[20] D. Tian, Y. Li, D. Qu, X. Jin, and C. Chien, Appl. Phys. Lett. **106**, 212407 (2015).
[21] S. M. Wu, J. Hoffman, J. E. Pearson, and A. Bhattacharya, Appl. Phys. Lett. **105**, 092409 (2014).
[22] Y. Xu, B. Yang, C. Tang, Z. Jiang, M. Schneider, R. Whig, and J. Shi, Appl. Phys. Lett. **105**, 242404 (2014).
[23] C. Du, H. Wang, F. Yang, and P. C. Hammel, Phys. Rev. Applied **1**, 044004 (2014).
[24] P. Bougiatioti, C. Klewe, D. Meier, O. Manos, O. Kuschel, J. Wollschläger, L. Bouchenoire, S. D. Brown, J.-M. Schmalhorst, G. Reiss *et al.*, Phys. Rev. Lett. **119**, 227205 (2017).
[25] See Supplemental Material at http://link.aps.org/supplemental/10.1103/PhysRevLett.124.017203 for details, which includes Refs. [26–29].
[26] J. L. Cohn, J. J. Neumeier, C. P. Popoviciu, K. J. McClellan, and T. Leventouri, Phys. Rev. B **56**, R8495 (1997).
[27] W. Schnelle, R. Fischer, and E. Gmelin, J. Phys. D **34**, 846 (2001).
[28] M. T. Buscaglia, F. Maglia, U. Anselmi-Tamburini, D. Marré, I. Pallecchi, A. Ianculescu, G. Canu, M. Viviani, M. Fabrizio, and V. Buscaglia, J. Eur. Ceram. Soc. **34**, 307 (2014).
[29] D. T. Morelli, J. Mater. Res. **7**, 2492 (1992).
[30] H. Wang, C. H. Du, Y. Pu, R. Adur, P. C. Hammel, and F. Y. Yang, Phys. Rev. Lett. **112**, 197201 (2014).
[31] G. Campillo, A. Berger, J. Osorio, J. Pearson, S. Bader, E. Baca, and P. Prieto, J. Magn. Magn. Mater. **237**, 61 (2001).
[32] G. J. Snyder, R. Hiskes, S. DiCarolis, M. R. Beasley, and T. H. Geballe, Phys. Rev. B **53**, 14434 (1996).
[33] V. Castel, N. Vlietstra, J. Ben Youssef, and B. J. van Wees, Appl. Phys. Lett. **101**, 132414 (2012).
[34] C. Du, H. Wang, P. C. Hammel, and F. Yang, J. Appl. Phys. **117**, 172603 (2015).
[35] J. Xiao, G. E. W. Bauer, K. C. Uchida, E. Saitoh, and S. Maekawa, Phys. Rev. B **81**, 214418 (2010).
[36] S. M. Rezende, R. L. Rodríguez-Suárez, R. O. Cunha, A. R. Rodrigues, F. L. A. Machado, G. F. Guerra, J. C. L. Ortiz, and A. Azevedo, Phys. Rev. B **89**, 014416 (2014).

[37] M. Arana, M. Gamino, E. Silva, V. Barthem, D. Givord, A. Azevedo, and S. Rezende, Phys. Rev. B **98**, 144431 (2018).
[38] S. R. Marmion, M. Ali, M. McLaren, D. A. Williams, and B. J. Hickey, Phys. Rev. B **89**, 220404(R) (2014).
[39] Y. M. Lu, Y. Choi, C. M. Ortega, X. M. Cheng, J. W. Cai, S. Y. Huang, L. Sun, and C. L. Chien, Phys. Rev. Lett. **110**, 147207 (2013).
[40] S.-Y. Huang, X. Fan, D. Qu, Y. Chen, W. Wang, J. Wu, T. Chen, J. Xiao, and C. Chien, Phys. Rev. Lett. **109**, 107204 (2012).
[41] J. Barker and G. E. W. Bauer, Phys. Rev. Lett. **117**, 217201 (2016).
[42] H. Adachi, Y. Yamamoto, and M. Ichioka, J. Phys. D **51**, 144001 (2018).
[43] S. Taran, B. Chaudhuri, S. Chatterjee, H. Yang, S. Neeleshwar, and Y. Chen, J. Appl. Phys. **98**, 103903 (2005).
[44] A. Berger, G. Campillo, P. Vivas, J. Pearson, S. Bader, E. Baca, and P. Prieto, J. Appl. Phys. **91**, 8393 (2002).
[45] M. Isasa, E. Villamor, L. E. Hueso, M. Gradhand, and F. Casanova, Phys. Rev. B **91**, 024402 (2015).
[46] P. Dai, J. A. Fernandez-Baca, E. W. Plummer, Y. Tomioka, and Y. Tokura, Phys. Rev. B **64**, 224429 (2001).
[47] V. Dyakonov, V. Shapovalov, E. Zubov, P. Aleshkevych, A. Klimov, V. Varyukhin, V. Pashchenko, V. Kamenev, V. Mikhailov, K. Dyakonov, V. Popov, S. J. Lewandowski, M. Berkowski, R. Zuberek, A. Szewczyk, and H. Szymczak, J. Appl. Phys. **93**, 2100 (2003).
[48] B. Heinrich, C. Burrowes, E. Montoya, B. Kardasz, E. Girt, Y.-Y. Song, Y. Sun, and M. Wu, Phys. Rev. Lett. **107**, 066604 (2011).
[49] H. Nakayama, K. Ando, K. Harii, T. Yoshino, R. Takahashi, Y. Kajiwara, K.-i. Uchida, Y. Fujikawa, and E. Saitoh, Phys. Rev. B **85**, 144408 (2012).
[50] T. K. H. Pham, M. Ribeiro, J. H. Park, N. J. Lee, K. H. Kang, E. Park, V. Q. Nguyen, A. Michel, C. S. Yoon, S. Cho *et al.*, Sci. Rep. **8**, 13907 (2018).
[51] C. Swindells, A. T. Hindmarch, A. J. Gallant, and D. Atkinson, Phys. Rev. B **99**, 064406 (2019).
[52] W. Cao, L. Yang, S. Auffret, and W. E. Bailey, Phys. Rev. B **99**, 094406 (2019).
[53] A. Ghosh, S. Auffret, U. Ebels, and W. E. Bailey, Phys. Rev. Lett. **109**, 127202 (2012).
[54] C. L. Jermain, S. V. Aradhya, N. D. Reynolds, R. A. Buhrman, J. T. Brangham, M. R. Page, P. C. Hammel, F. Y. Yang, and D. C. Ralph, Phys. Rev. B **95**, 174411 (2017).